

Inhibitory effects of salidroside on MCF-7 breast cancer cells *in vivo*

Journal of International Medical Research

48(11) 1–12

© The Author(s) 2020

Article reuse guidelines:

sagepub.com/journals-permissions

DOI: 10.1177/0300060520968353

journals.sagepub.com/home/imrAn-Qi Sun^{1,2}  and Xiu-Lian Ju¹

Abstract

Objective: We investigated the antitumor effects of salidroside and preliminarily examined its underlying mechanisms by establishing a nude mouse model bearing MCF-7 breast cancer cell xenografts.

Methods: The mice were grouped and intraperitoneally injected with salidroside, paclitaxel, or physiological saline. Tumor samples were weighed, and immunohistochemical staining with hematoxylin and eosin and anti-CD34 antibody was performed. Tumor cell apoptosis was observed using the terminal deoxynucleotidyl transferase deoxyuridine dUTP nick end labeling assay. Bcl-1, p53, Bax, and caspase 3 expression in tumor tissues was determined via western blotting.

Results: The tumor inhibition rate of high-dose salidroside was 75.16%, which was significantly higher than the rates for paclitaxel and saline. A tumor tissue pathology analysis revealed that high-dose salidroside inhibited tumor cell proliferation and promoted tumor cell apoptosis. Western blotting revealed that Bcl-2 and p53 expression were significantly lower in the salidroside group than in the other groups, whereas Bax and caspase 3 (17 kDa) expression were increased.

Conclusions: Salidroside was more effective than paclitaxel in inhibiting tumor growth in MCF-7 breast cancer cell-bearing nude mice. The mechanism of action may involve Bcl-2 and p53 down-regulation and Bax and caspase 3 upregulation, thereby increasing proapoptotic factor expression and inducing tumor cell apoptosis.

¹Key Laboratory for Green Chemical Process of Ministry of Education, School of Chemical Engineering & Pharmacy, Wuhan Institute of Technology, Wuhan, People's Republic of China

²The College of Post and Telecommunication, Wuhan Institute of Technology, Wuhan, People's Republic of China

Corresponding author:

Xiu-Lian Ju, Key Laboratory for Green Chemical Process of Ministry of Education, School of Chemical Engineering & Pharmacy, Wuhan Institute of Technology, 366 Huquan Street, Wuhan 430073, People's Republic of China.
Email: xiulianju2001@yahoo.com



Keywords

Salidroside, breast cancer, antitumor, apoptosis, xenograft, nude mice, MCF-7 cells

Date received: 27 May 2020; accepted: 29 September 2020

Introduction

Breast cancer is a malignant tumor with a high incidence in women and a significantly increasing incidence in developed and developing countries globally, and it severely threatens the health of women.¹ Therefore, it is vital to identify effective preventative and treatment measures. Currently, there is a preference for molecular targeted drugs for the treatment of breast cancer.² The clinical application of different chemotherapeutics has significantly increased the cure rates of tumors and prolonged patient survival. However, chemotherapy consists mainly of synthesized drugs, which are expensive to develop and which are associated with toxicity and immunosuppression, leading to serious toxic side effects in healthy body tissues. Therefore, the development of effective and safe antitumor drugs is currently the most important goal. Traditional Chinese medicine (TCM) formulations have direct cytotoxic or inhibitory effects on tumor cells. They also alleviate signs and symptoms in patients and increase the efficacy of chemotherapy.³

Preclinical investigations regarding TCM are usually fragmentary and are often not comparable because of the use of different extracts and administration, but it is important to explore the mechanism of action of the active ingredients in the herbs. Salidroside is the main active ingredient in *Rhodiola rosea* L. grass or its roots and stems.^{4,5} *In vitro* experiments demonstrated that salidroside inhibits the proliferation of many types of cancer cells (HeLa human cervical cancer, SPC-A-1 lung adenocarcinoma, QGY-7703 liver cancer, and TEU-2

bladder cancer cells⁶⁻¹⁰). Furthermore, a study found that salidroside inhibits breast cancer cell growth and induces apoptosis *in vitro*.¹¹

To further study the antitumor effects of salidroside, a nude mouse model bearing MCF-7 breast cancer cells was established. Furthermore, we used a standard breast cancer drug, paclitaxel, as a positive control to examine the inhibitory effects of salidroside on breast cancer cells *in vivo*. Finally, we preliminarily examined the underlying mechanisms.

Materials and methods

Establishment of the animal model

Forty specific pathogen-free female BALB/C-nu mice weighing 16 to 20 g were purchased from SJA Laboratory Animal Co., Ltd (Hunan, China). The MCF-7 human breast cancer cell line was purchased from Biofavor Biotechnology Co., Ltd (Wuhan, China). After a 7-day acclimatization period, cotton balls containing alcohol were used to disinfect the skin of the right forelimb of each animal. MCF-7 cells at the logarithmic phase were collected and subcutaneously inoculated into the right forelimbs of nude mice (1×10^6 to 1×10^7 cells/mouse in a volume of 200 μ L). Then, the inoculation site was gently pressed to prevent cells from escaping, and the mice were returned to their cages for routine housing. Tumorigenesis was confirmed when subcutaneous tumor nodules with a hard texture were observed at the inoculation site.

Hubei Provincial Center for Disease Control and Prevention approved this research (SYXK2017-0065, Hubei, 2017.6.). We have taken adequate care of the animals in reference to the ARRIVE guidelines and made efforts to minimize the number of animals utilized and decrease their suffering.

Drug administration method and dose

Salidroside (99.9%) was purchased from Synchallenge Unipharm Inc., Ltd (Wuhan, China), and paclitaxel was purchased from Wuhan Biocata Biological Technology Co., Ltd (Wuhan, China). Tumor growth was observed daily, and when the tumors had grown to a volume of 100 to 150 mm³, the mice were randomized into the five groups of eight mice each as follows: 1) blank control (physiological saline); 2) positive control (2 mg/kg paclitaxel); 3) low-dose salidroside (20 mg/kg); 4) medium-dose salidroside (40 mg/kg); and 5) high-dose salidroside (80 mg/kg). Drugs were administered via intraperitoneal injection to the mice in a volume of 0.2 mL per mouse continuously for 8 days.

Measurement and sample collection

Starting on day 3 after drug administration, Vernier calipers were used to measure the long and short diameters of the tumors until the end of the experiment. Tumor volume was measured using the following formula: $V = (a \times b^2)/2$, where a and b are the long and short diameters of the tumor, respectively. The mice were euthanized via cervical dislocation, and the tumors were weighed to calculate the tumor inhibition rate (IR, %) as follows: $IR = [1 - (\text{weight of tumor mass from the experimental group} / \text{weight of tumor mass from the control group})] \times 100$. Tumor masses were extracted, arranged by group on a piece of white paper, photographed, fixed in 4%

paraformaldehyde, and preserved for subsequent experiments.

Hematoxylin and eosin (H&E) staining

Fixed tumor tissue blocks were trimmed before ethanol dehydration and tissue clearing to permit the paraffin to effectively penetrate the cells. The paraffin wax-embedded tissue blocks were sectioned, dried, and stained with H&E for pathological examination. A microscope was used to photograph the sections at $\times 200$ magnification to observe the tumor tissue pathology and structural changes.

CD34 immunohistochemical staining to observe tumor blood vessels

The paraffin sections were dewaxed, and antigen retrieval was performed. Briefly, the tissue sections were incubated with 3% hydrogen peroxide to block endogenous peroxidases, followed by blocking with dilute goat serum at 25°C for 30 minutes to reduce non-specific staining. Then, the tissues were sequentially incubated with primary antibodies, enzyme-labeled secondary antibodies, and the chromogenic agent, followed by hematoxylin counterstaining, dehydration, and mounting. Weidner's calibration method, in which the two regions (hotspots) with the most microvessels were selected under low magnification ($\times 10$) for each sample, was used. The number of microvessels was counted in four fields for every region under $\times 40$ magnification, and the microvessel density was calculated.

Terminal deoxynucleotidyl transferase deoxyuridine dUTP nick end labeling (TUNEL) assay

Tumor tissues were embedded in paraffin, sectioned, washed with phosphate-buffered saline (PBS), fully immersed in 20 $\mu\text{g}/\text{mL}$ proteinase K solution, and then incubated

at room temperature for 20 minutes. Deionized water was used to dilute 5× equilibration buffer by 5-fold, and then each tissue sample, including the test region of interest, was covered with 100 mL of 1× equilibration buffer and incubated at room temperature for 10 to 30 minutes. The glass slides were placed in a wet box, which was wrapped in aluminum foil to protect it from light and then incubated at 37°C for 60 minutes. The slides were then washed with PBS thrice for 5 minutes each, followed by incubation with DAPI in the dark for 5 minutes for nuclear staining. PBS plus Tween 20 (PBST) was used to wash the slides four times for 5 minutes each. Absorbent paper was used to remove excess liquid from the sections, which were then mounted with anti-fade mounting solution, and images were observed and acquired using a fluorescent microscope.

Western blotting

Proteins were extracted from tumor tissues, and a regression equation was used to calculate the protein concentration of the samples. The extracted proteins were denatured before cooling to room temperature and stored at -20°C. A polyacrylamide gel electrophoresis (PAGE) gel was cast and placed in the electrophoresis tank. A micropipette was used to load the protein samples (40 µg each) and marker into the wells. The target bands were cut from the gel based on the markers and washed with distilled water. Polyvinylidene fluoride (PVDF) membranes and filter papers of the same size as the PAGE gel were cut, and after the PVDF membranes were soaked in methanol for several minutes, they were immersed in transfer buffer with filter paper.

Tris-buffered saline plus Tween (TBST, blocking solution) containing 5% skimmed milk was used to block the PVDF

membranes for 2 hours at room temperature with shaking. The PVDF membranes were then incubated with the corresponding primary antibodies diluted in blocking solution at 4°C overnight. This was followed by thorough washing five to six times for 5 minutes each. Horseradish peroxidase-labeled secondary antibodies were diluted in blocking solution to 1:5000 and then incubated with the PVDF membranes at 37°C for 2 hours with shaking. TBST was used to thoroughly wash the PVDF membranes five to six times for 5 minutes each.

The enhancer solution in the enhanced chemiluminescence kit was mixed with the peroxidase solution at a 1:1 ratio. The working solution was added to the PVDF membrane and allowed to react for a few minutes, during which the fluorescent bands were visible, and then filter paper was used to absorb the excess substrate solution. The membrane was covered with plastic wrap, which was then covered with the X-ray film, followed by the developing solution and then the fixer solution. Finally, the films were rinsed, dried, and scanned, and then BandScan (Glyko Inc., Novato, CA, USA) was used to analyze the grayscale values of the developed films.

Statistical analysis

Quantitative data were expressed as the mean ± standard deviation), and Statistical Package for the Social Sciences version 17.0 (IBM, Armonk, NY, USA) was used to perform analysis of variance.

Results

Tumor growth inhibition status

In nude mice bearing MCF-7 cell xenografts, tumor growth was significantly inhibited by salidroside. High-dose salidroside exhibited the strongest antitumor effects, and the differences in tumor

volume and mass between the high-dose salidoside and blank control groups were statistically significant (both $P < 0.05$). The tumor IRs in the paclitaxel and high-dose salidoside groups were 61.86 and 75.16%, respectively ($P < 0.05$). Figure 1 and Table 1 present the tumor sizes, growth curves, and tumor IRs.

Pathological and structural changes in tumor tissues

H&E staining. H&E staining was used to observe the pathological changes in tumor tissues, and the results are presented in Figure 2. In the blank control group, tumor cells exhibited dense arrangement and cellular atypia, and tumor tissues in the middle of the section displayed marked growth. Compared with the findings in the blank control group, large necrotic areas were observed in the positive control and high-dose salidoside groups.

These tumor tissues were loose, they had an irregular cell arrangement, and the number of cells was significantly decreased. In the other treatment groups, tumor cells exhibited a sparse arrangement, and necrotic areas were observed.

Immunohistochemical detection of CD34. Immunohistochemical detection of CD34 in tumor tissues was conducted, as presented in Figure 3. As presented in Table 2, the differences in microvessel density among the high-dose salidoside, positive control, and blank control groups were statistically significant ($P < 0.05$). This illustrated that salidoside significantly reduced microvessel density and inhibited angiogenesis in tumors, thereby inhibiting their growth.

TUNEL assay. We established a breast cancer mouse model and used the TUNEL assay to quantitate tumor cell apoptosis

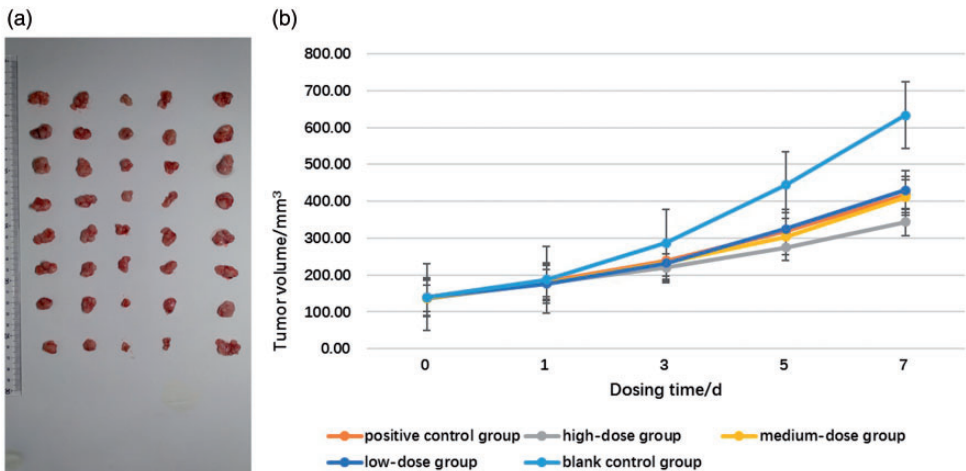


Figure 1. Effects of salidoside on tumor size and growth curve in mice. (a) Effect of salidoside on tumor size in mice. From left to right are the low-dose salidoside group, middle-dose salidoside group, high-dose salidoside group, positive control group, and blank control group. Tumor size was smaller in the salidoside groups than in the blank control group, and high-dose salidoside had the strongest antitumor effects. (b) Tumor growth curve. The differences in tumor volume and mass between the high-dose salidoside and blank control groups were statistically significant (both $P < 0.05$). In nude mice bearing MCF-7 cell xenografts, tumor growth was significantly inhibited in the salidoside groups. High-dose salidoside displayed the best antitumor effects.

Table 1. Tumor weight and inhibition rates (n = 8).

Variables	Blank control	Positive control	High-dose salidroside	Medium-dose salidroside	Low-dose salidroside
Tumor weight (g)	1.180 ± 0.0778	0.450 ± 0.112	0.293 ± 0.102	0.835 ± 0.143	1.065 ± 0.0542
Tumor inhibition rate	0.00%	61.86%*	75.16%*#	29.28%*#	9.74%*#

*compared with blank control group, $P < 0.05$.

#compared with positive control group, $P < 0.05$.

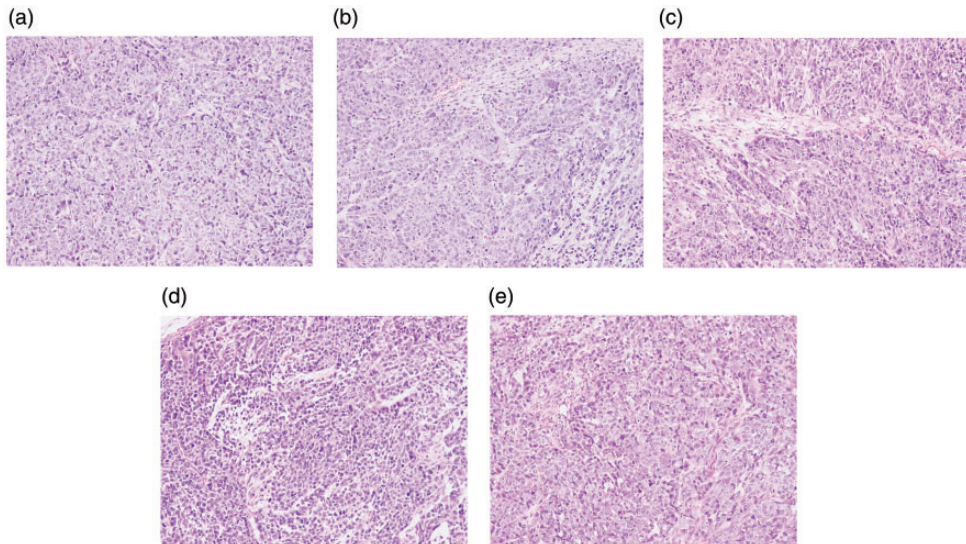


Figure 2. Pathological changes of tumor tissue after hematoxylin and eosin staining ($\times 200$). (a) Blank control group, (b) positive control group, and (c, d, and e) samples treated with high-, medium-, and low-dose salidroside, respectively. Compared with the blank control, large necrotic areas were observed in tissues treated with the positive control and high-dose salidroside. These tumor tissues were loose, they had an irregular cell arrangement, and the number of cells was significantly decreased. In the other treatment groups, tumor cells displayed a sparse arrangement, and necrotic areas were observed.

(Figure 4). Compared with the findings in the blank control group, the number of apoptotic cells was significantly increased in all treatment groups, with significant apoptosis observed in the positive control and high-dose salidroside groups.

We selected three high-magnification fields ($\times 400$) and counted all cells in each field to calculate the labeling index as the

number of positive cells in each field divided by the total number of cells in the field. The apoptosis index of each group was equal to the mean labeling index for each field. As presented in Table 3, the apoptotic indices in the positive control and high-dose salidroside groups were significantly different from that in the blank control group (both $P < 0.05$).

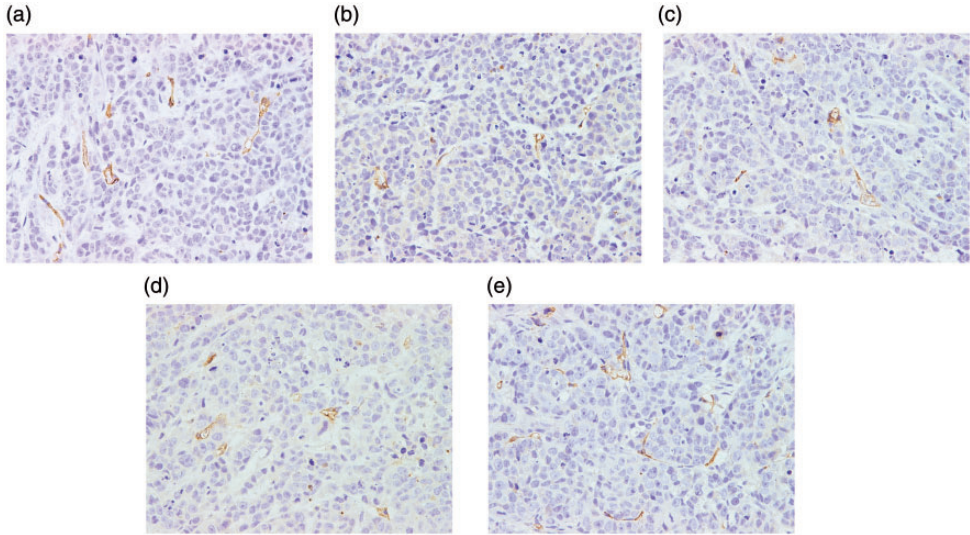


Figure 3. Immunohistochemical staining for CD34 on tumor blood vessels ($\times 400$). (a) Blank control group, (b) positive control group, and (c, d, and e) samples treated with high-, medium-, and low-dose salidroside, respectively. Salidroside significantly reduced microvessel density and inhibited angiogenesis in tumors.

Table 2. Analysis of microvessels via immunohistochemical staining for CD34.

Groups	Sample	Field 1	Field 2	Field 3	Field 4	Average	MVD
Blank control	1	14	16	14	15	14.750	21.833
	2	34	29	33	16	28.000	
	3	24	37	18	12	22.750	
Positive control	1	7	9	8	8	8.000	9.583*
	2	11	15	9	12	11.750	
	3	11	9	6	10	9.000	
High-dose salidroside	1	6	12	11	8	9.250	8.250*
	2	11	13	8	10	10.500	
	3	3	4	7	6	5.000	
Medium-dose salidroside	1	13	14	12	15	13.500	12.833
	2	9	15	9	11	11.000	
	3	12	18	10	16	14.000	
Low-dose salidroside	1	13	24	12	11	15.000	15.000
	2	14	16	13	20	15.750	
	3	12	15	16	14	14.250	

*compared with blank control group, $P < 0.05$.

MVD, microvessel density.

Western blot quantitation of protein expression in MCF-7 breast cancer cells. The results revealed that Bcl-2 and p53 protein expression was significantly lower in the

salidroside and positive control groups than in the blank control group (both $P < 0.05$), whereas Bax and caspase 3 (17 kDa) levels were significantly higher in

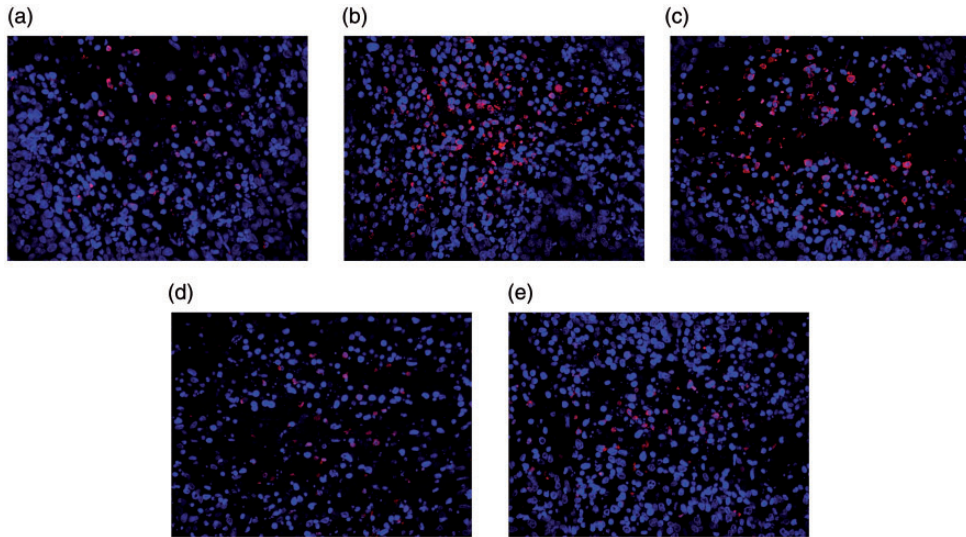


Figure 4. (a) Blank control group, (b) positive control group, and (c, d, and e) samples treated with high-, medium-, and low-dose solidoside, respectively. Compared with the effects of the blank control, the number of apoptotic cells was significantly increased in all treatment groups, with significant apoptosis present in (b) and (c).

Table 3. Apoptotic index.

Group	Number of apoptotic cells	Total number of cells	Apoptotic rate	Apoptotic index	Average value
Blank control group 1	29	371	7.82%	6.67%	5.30%
	32	741	4.32%		
	19	241	7.88%		
Blank control group 2	34	921	3.69%	4.78%	
	57	1035	5.51%		
	51	994	5.13%		
Blank control group 3	47	985	4.77%	4.45%	
	21	482	4.36%		
	38	899	4.23%		
Positive control group 1	75	1052	7.13%	7.36%	10.68%*
	47	984	4.78%		
	87	856	10.16%		
Positive control group 2	189	1065	17.75%	12.95%	
	142	1452	9.78%		
	137	1211	11.31%		
Positive control group 3	124	1245	9.96%	11.75%	
	141	1194	11.81%		
	154	1142	13.49%		
High-dose group 1	124	1385	8.95%	10.51%	10.41%*
	133	1176	11.31%		
	115	1022	11.25%		

(continued)

Table 3. Continued.

Group	Number of apoptotic cells	Total number of cells	Apoptotic rate	Apoptotic index	Average value
High-dose group 2	84	1321	6.36%	8.55%	
	135	1256	10.75%		
	112	1309	8.56%		
High-dose group 3	158	692	22.83%	12.17%	
	83	951	8.73%		
	61	1235	4.94%		
Medium-dose group 1	68	1089	6.24%	7.87%	6.60%
	72	805	8.94%		
	116	1377	8.42%		
Medium-dose group 2	74	1597	4.63%	6.49%	
	62	1485	4.18%		
	91	853	10.67%		
Medium-dose group 3	49	901	5.44%	5.42%	
	57	878	6.49%		
	63	1452	4.34%		
Low-dose group 1	35	1315	2.66%	4.82%	4.98%
	67	1605	4.17%		
	124	1624	7.64%		
Low-dose group 2	48	1203	3.99%	5.42%	
	79	1459	5.41%		
	91	1327	6.86%		
Low-dose group 3	6	935	0.64%	4.69%	
	62	1557	3.98%		

* compared with blank control group, $P < 0.05$.

the treatment groups (both $P < 0.05$). Conversely, caspase 3 (35 kDa) expression was lower in the treatment groups than in the blank control group, but these differences were not significant (Table 4 and Figure 5).

Discussion

The cytotoxic effects of antitumor drugs on breast cancer cells may be mediated through multiple pathways such as inhibition of cell cycle progression, induction of cellular apoptosis, inhibition of cell migration, reversal of drug resistance, and alteration of gene expression, and these drugs have wide application prospects. In addition, it is important to establish a suitable

animal model of breast cancer to study its biological behavior and develop new treatments.^{12–16} However, there are few local and global reports on the inhibitory effects of salidroside on breast cancer cells *in vivo*. To understand the molecular effects of salidroside and evaluate its efficacy *in vivo*, we establish an animal model and provided evidence that the drug strongly inhibits proliferation and induces apoptosis in MCF-7 breast cancer cells.

In this study, we observed that high doses of salidroside exerted significant inhibitory effects and had similar or stronger inhibitory effects than paclitaxel on MCF-7 cell growth *in vivo*. There were statistically significant differences in tumor volume and mass between the salidroside

Table 4. Protein expression (n = 3).

Protein	Blank control	Positive control	High-dose salidroside	Medium-dose salidroside	Low-dose salidroside
Bcl-2	0.477 ± 0.0778	0.247 ± 0.0207*	0.333 ± 0.0207*	0.398 ± 0.00958*	0.445 ± 0.00976*
Bax	0.256 ± 0.0308	0.484 ± 0.0200*	0.481 ± 0.0169*	0.426 ± 0.0240*	0.341 ± 0.0178*
p53	0.379 ± 0.0144	0.136 ± 0.0217*	0.150 ± 0.0335*	0.223 ± 0.0102*	0.295 ± 0.0172*
Caspase 3 (35 kDa)	0.507 ± 0.0190	0.506 ± 0.0245	0.505 ± 0.0150	0.498 ± 0.0427	0.504 ± 0.0345
Caspase 3 (17 kDa)	0.153 ± 0.0200	0.356 ± 0.0227*	0.381 ± 0.0398*	0.263 ± 0.0267*	0.217 ± 0.0222*

Data are presented relative to the expression of GAPDH, which was set as 1.

*compared with blank control group, $P < 0.05$.

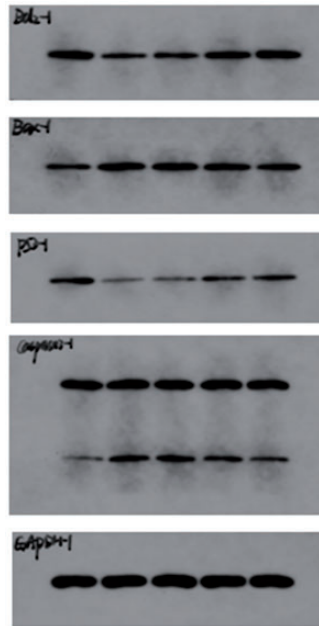


Figure 5. Expression of different proteins in MCF-7 cells. From left to right are the blank control group, positive control group, high-dose salidroside group, middle-dose salidroside group, and low-dose salidroside group. Salidroside decreased Bcl-2 and p53 expression and increased Bax and caspase 3 expression.

and blank control groups, and the drug more strongly suppressed tumor growth than paclitaxel. H&E staining was used to analyze pathological and structural changes in tumor tissues. We observed that tumor tissues in the high-dose salidroside group exhibited large areas of cell rupture, cell loss, and infiltration of inflammatory cells.

This illustrated that salidroside inhibited the proliferation of tumor cells. The formation of tumor blood vessels promotes tumor growth. The result that high-dose salidroside significantly inhibited angiogenesis in mouse tumors indicated antiangiogenesis may be one of its antitumor mechanisms. Coupled with the findings in the TUNEL

assay, these results indicate that high doses of salidroside significantly promoted cell apoptosis. Therefore, salidroside inhibited tumor cell proliferation and promoted apoptosis, which are beneficial for restoring the normal ratio of cells undergoing proliferation and apoptosis.

We further studied the effector mechanisms by which salidroside exerted its inhibitory effects on tumor cells *in vivo*. We selected and quantified the protein products of relevant genes (*Bcl-2*, *p53*, *Bax*, and *Casp3*) in breast cancer research. Our preliminary results revealed that *Bcl-2* and *p53* downregulation and *Bax* and caspase 3 upregulation may be two mechanisms by which salidroside induces apoptosis of breast cancer cells.

This study had some limitations. For instance, the dosage should be validated scientifically, and the sample size should be increased. To further investigate the potential antitumor effects of salidroside on breast cancer cells, we plan to use MDA-MB-231 cells as models to study the possible molecular mechanisms. In summary, additional research is needed before clinical utility can be suggested.

Conclusion

Salidroside is effective in inhibiting tumor growth in MCF-7 breast cancer cell-bearing nude mice. The mechanism of action may involve downregulating *Bcl-2* and *p53*, and upregulating *Bax* and caspase 3, thereby increasing pro-apoptotic factor expression and inducing tumor cell apoptosis. Therefore, salidroside may be a promising candidate for breast cancer treatment, and it is important to further study the molecular effects of salidroside and evaluate its efficacy.

Acknowledgement

We acknowledge Ms. Xian-Ju Huang for helpful suggestions and proofreading.


Declaration of conflicting interest

The authors declare that there is no conflict of interest.

Funding

This study was supported by the Research Project of Hubei Provincial Department of Education (No. B2018429).

ORCID iD

An-Qi Sun  <https://orcid.org/0000-0002-7050-2423>

References

1. Higgs MJ and Baselga J. Targeted therapies for breast cancer. *J Clin Invest* 2011; 121: 3797–3803.
2. Sertel S, Plinkert PK and Efferth T. Natural Products Derived from Traditional Chinese Medicine as Novel Inhibitors of the Epidermal Growth Factor Receptor. *Comb Chem High Throughput Screen* 2010; 13: 849–854.
3. Li J, Lin HS, Wang XT, et al. The molecular mechanism of traditional Chinese medicine resculpture effect on the process of tumor immunoeediting. *World Sci Tch* 2009; 11: 747–752.
4. Chiang HM, Chen HC, Wu CS, et al. Rhodiola plants: Chemistry and biological activity. *J Food Drug Anal* 2015; 23: 359–369.
5. Hu XL, Lin SX, Yu DH, et al. A preliminary study: the anti-proliferation effect of salidroside on different human cancer cell lines. *Cell Biol Toxicol* 2010; 26: 499–507.
6. Liu ZB, Li XS, Simoneau AR, et al. Rhodiola roesa extracts and Salidroside decrease the growth of bladder cancer cell lines via inhibition of the mTOR pathway and induction of induction of autophagy. *Mol Carcinog* 2012; 51: 257–267.
7. Sun C, Wang ZH and Zheng QS. Salidroside inhibits migration and invasion of human fibrosarcoma HT1080 cells. *Phytomedicine* 2012; 19: 355–363.
8. Yan DM, Dai RY, Duan CY, et al. Cross-talk between PI3K/Akt and MEK/ERK pathways regulates human hepatocellular

- carcinoma cell cycle progression under endoplasmic reticulum stress. *Chinese J Hepatology* 2010; 18: 909–914.
9. Tomek K, Wagner R, Varga F, et al. Blockade of fatty acid synthase induces ubiquitination and degradation of phosphoinositide-3-kinase signaling proteins in ovarian cancer. *Mol Cancer Res* 2011; 9: 1767–1779.
 10. Wan J, Wu W, Chen Y, et al. Insufficient radiofrequency ablation promotes the growth of non-small cell lung cancer cells through PI3K/Akt/HIF-1 α signals. *Acta Biochimica Et Biophysica Sinica* 2016; 48: 371–377.
 11. Hu XL, Zhang XQ, Qiu SF, et al. Salidroside induces cell-cycle arrest and apoptosis in human breast cancer cells. *Biochem Biophys Res Commun* 2010; 398: 62–67.
 12. Hutchinson JN and Muller WJ. Transgenic mouse models of human breast cancer. *Oncogene* 2000; 19: 6130–6137.
 13. Zhang JP, Liu AH and Hou RR. Salidroside protects cardiomyocyte against hypoxia-induced death: A HIF-1 α -activated and VEGF-mediated pathway. *Eur J Pharmacol* 2009; 607: 6–14.
 14. Xu ZW, Chen X and Jin XH. SILAC-based proteomic analysis reveals that salidroside antagonizes cobalt chloride-induced hypoxic effects by restoring the tricarboxylic acid cycle in cardiomyocytes. *J Proteomics* 2016; 130: 211–220.
 15. Guney T, Kohles SA and Thompson VL. Heterocycles from wine: synthesis and biological evaluation of salidrosides. *Tetrahedron* 2015; 71: 3115–3119.
 16. Sun KX, Xia HW and Xia RL. Anticancer effect of salidroside on colon cancer through inhibiting JAK2/STAT3 signaling pathway. *Int J Clin Exp Pathol* 2015; 8: 615–621.